

A hybrid vanadium redox/lithium-ion energy storage system for off-grid renewable power

Leong Kit Gan, Jorn Reniers and David Howey

Department of Engineering Science, University of Oxford, Oxford, United Kingdom

Email: leong.gan@eng.ox.ac.uk, jorn.reniers@stx.ox.ac.uk and david.howey@eng.ox.ac.uk

Abstract—In off-grid renewable power systems, batteries are often used to balance the mismatch between load and electricity generation. The mismatch may be more severe in small-scale systems due to the lack of averaging effect seen in larger power systems. In the former, batteries have to cope with rapid power fluctuations whilst still delivering power to consumers. A vanadium redox flow battery (VRB) may seem to be an ideal energy storage system in this case due to its well-known durability and ease of expanding its energy capacity. However, the associated parasitic losses used for electrolyte circulation will dominate when the charge/discharge power is low, and this is particularly inefficient when no other means of energy storage is available. This work proposes the hybridisation of VRB and lithium-ion batteries (LIBs), which complement one another in terms of energy capacity, power handling capability and durability. The trade-off between the parasitic losses of VRB vs. the degradation of LIB presents an interesting optimisation problem. To investigate this, a VRB system which consists of a stack model and a mechanical model was developed before establishing an appropriate energy management system (EMS) using a conventional rule-based approach. In addition, a mixed integer linear programming technique was used to solve the multi-objective optimisation problem in order to investigate the operation of the proposed hybrid energy storage system (HESS) using realistic solar irradiance and load demand profiles. A sensitivity analysis was conducted with different weights for the two objectives. A high-fidelity physical model (Matlab/Simulink) was used to study the underlying transients and to validate the control strategies.

Index Terms—Hybrid energy storage, flow battery, lithium-ion, off-grid, optimisation, photovoltaics.

I. INTRODUCTION

Traditionally, off-grid power systems rely on diesel generators to supply remote areas where a grid connection is not available. The use of diesel generators in these remote locations has proven to be uneconomical due to the difficult terrain which translates into high fuel transportation costs [1]. Recent developments in off-grid renewable energy systems which use natural resources such as wind, photovoltaics (PV) or hydro, and energy storage systems (ESSs), have decreased reliance on diesel generators. Many research activities now focus on the development of new battery and super-capacitor (SC) technology, usually aiming at enhancing the power or energy capacity [2] of an ESS. However, despite significant improvements, an ultimate all-rounder technology which transcends all aspects such as cost, efficiency, power/energy capacity, weight/volume, cycle life, etc. is not available [2]. A hybrid ESS (HESS), which typically consists of different

energy storage elements, each having different characteristics, has the potential to overcome the limitations of a single-technology ESS by exploiting only the combined advantages while minimising disadvantages [2].

Lead-acid batteries (LABs) and lithium-ion batteries (LIBs) are popular choices to support off-grid systems. Despite their advantages and availability, the lifetime of these batteries is limited, and they may not be ideal to serve a large community with many battery banks. A more commercially beneficial and longer life solution may be to hybridise the system using different technologies. Most of the literature has been dedicated to hybridisation between SCs and batteries, e.g. [3]. It has been shown [4] that a control strategy for a SC-LAB HESS can be developed with the aim of improving the battery lifetime in a small-scale off-grid wind power system. It has been quantified that the battery life increases by diverting rapid power variations caused by wind turbulence and short-term load variations to the SC module [4].

This paper proposes the use of a vanadium redox flow battery (VRB) hybridised with lithium-ion batteries for an off-grid PV scenario. We developed two different energy management system (EMS) approaches for this HESS both of which are described in this paper. The overall aim is to trade-off the advantages and disadvantages of the two battery types. A VRB system is known to be durable, lasting in excess of 20,000 cycles [5], significantly more than standard lithium-ion cells [6]. Also, the energy capacity can be increased separately from the power capability by simply using larger tanks to store electrolyte [7]. Therefore whereas the economics of lithium-ion systems are optimal for relatively short time scales (e.g. a couple of hours), VRBs may be optimal for longer time scales, e.g. up to a day. Also, whilst lithium-ion cells are efficient because of their low impedance and low self-discharge, VRBs have higher ohmic losses and parasitic losses from the temperature regulation systems and the external pumps used for circulating the electrolyte [7]. Hence, a VRB-only ESS may not be the preferred option to supply an off-grid system because when charge/discharge power is low, the losses and parasitic loads will dominate. The integration of LIBs into the system, forming a HESS, is a sensible solution.

The following sections of this paper give an overview of the simulation approach (section II) and component modelling (section III), and then discuss two different control approaches (sections IV and V), followed by results, discussion and conclusions (sections VI and VII).

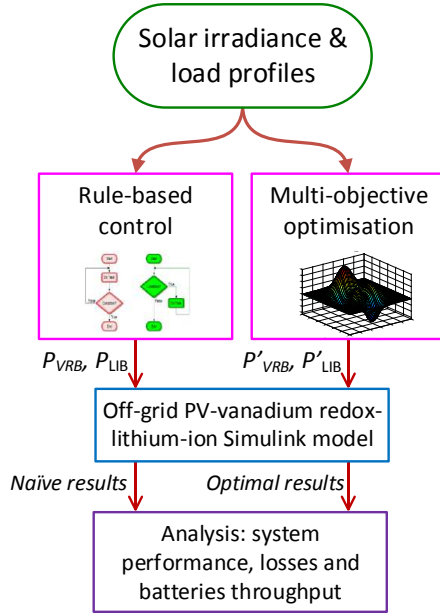


Fig. 1. Simulation methodology

II. SIMULATION METHODOLOGY

In order to explore the behaviour of a VRB/LIB HESS, including stability, we required realistic simulation models of the storage systems and converters. For this purpose we chose to use high fidelity models that run at $50 \mu s$ sampling time. The overall simulation methodology is presented in Fig. 1.

Since this work considers the short-term as well as longer term impacts of fluctuations in renewable energy generation, high-resolution (30-100Hz) solar irradiance time series data was used in the Simulink simulation [8]. As measured load data were not freely available, this work adopted an open-source bottom-up domestic load model [9] which has been qualitatively validated [10].

In addition to the high fidelity simulation model, a one-minute resolution multi-objective optimisation model was formulated in order to explore the HESS control trade-offs between power losses and degradation. The load and generation data were averaged to reduce the sampling interval for this purpose. Numerical results from the optimisation model (power commands for VRB and LIB) were fed into the high resolution Simulink model, which ran for twenty-four hours simulation time. It took approximately three days to complete one such simulation using a computer with an Intel Core i7 3.60 GHz processor, 32 GB of RAM and 64-bit Windows operating system.

III. MODELLING

The overall micro-grid is shown in Fig. 2. Grid-forming inverters were used to form a three-phase isolated grid. The architecture plus steady-state and dynamic analyses of this system is presented in [11]. A three-phase ac load was connected to the ac bus of the inverters. The PV, VRB and LIB were connected to the dc bus via separate dc-dc power converters, each controlled as current sources. These are briefly explained

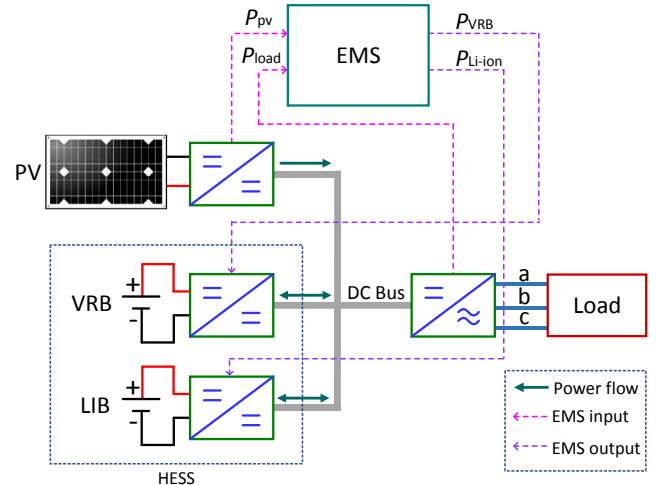


Fig. 2. Proposed HESS for standalone PV system

below for completeness. The Simulink built-in LIB and PV library models were used for the simulation, but a bespoke VRB model was developed. Most VRB modelling literature focuses on electrochemical simulation of unit cells and there are relatively few systems-level papers [12]. Since the VRB system architecture dictates its operational constraints and mechanical losses, a detailed understanding at the system level is important for designing the EMS control strategy.

A. Power converters and control schemes

In the simulation, the three-phase isolated grid was formed by three single-phase inverters, in which one unit works as the master and the other two units are slaves. Each inverter is rated at 6 kW. The well-known droop control strategy was adopted to emulate the conventional behaviour of a synchronous machine, controlling the voltage and frequency on the ac system [13]. An increase in active or reactive power demand is accompanied by a reduction in frequency or voltage, and vice versa. However, the difference between a power electronics-based inverter and a conventional synchronous machine is the absence of inertia in the former. Fortunately, power electronics is able to react to load variations quickly and therefore ensure a stable supply during transients, although this also requires the dc link capacitance and energy storage systems to be sized and controlled correctly.

Bi-directional half-bridge dc-dc converters were used to regulate the power from the VRB, LIB and PV panels. They were controlled as current sources with standard proportional-integral-based (PI) control loops. In order to extract maximum power from the PV panels, a maximum power pointing tracking (perturb and observe) algorithm [14] was adopted.

B. Vanadium redox flow battery system model

The VRB modelled in this work is based on a 19 cell, 2.5 kW / 5 kWh system, which was experimentally validated in the literature [15], which also gives dimensions, hydraulic and stack characteristics [16]. The top level VRB system

TABLE II
VRB SPECIFICATIONS [15]

$I_{stack} [pu]$	η_c	η_v
0	0	1.0
0.333	0.8255	0.9218
0.5	0.9138	0.8862
0.666	0.9452	0.8551
0.833	0.9468	0.8172
1.0	0.9640	0.7978

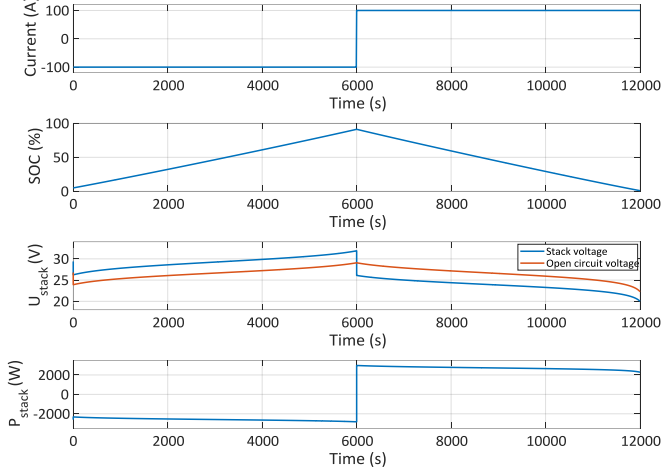


Fig. 5. Charge/discharge cycle of the modelled VRB stack

The pipe losses can be divided into major (main conduit) and minor (bends, elbows, valves) losses:

$$\Delta p_{pipe} = \rho g (h_{f,i} + h_{m,i}), \quad (6)$$

where $h_{f,i}$ is the friction loss and $h_{m,i}$ is the minor losses. The friction loss, $h_{f,i}$, can be calculated with the Darcy-Weisbach equation

$$h_{f,i} = f_i \frac{L_i}{D_i} \frac{V_{s,i}^2}{2g}, \quad (7)$$

where

- L length of pipes (m),
- D diameter of pipes (m),
- f friction factor,
- g gravitational acceleration (m/s^2),
- V_s fluid velocity (m/s).

The minor losses, $h_{m,i}$ can be determined with

$$h_{m,i} = k_{L,i} \frac{V_{s,i}^2}{2g}, \quad (8)$$

where $k_{L,i}$ are the minor loss coefficients [16].

The resulting mechanical model is shown in Fig. 6(a) and the simulated pump power consumption across different flow rates is shown in Fig. 6(b).

It is acknowledged that at a higher electrolyte flow rate, the voltage and coulombic efficiency increases but this comes at

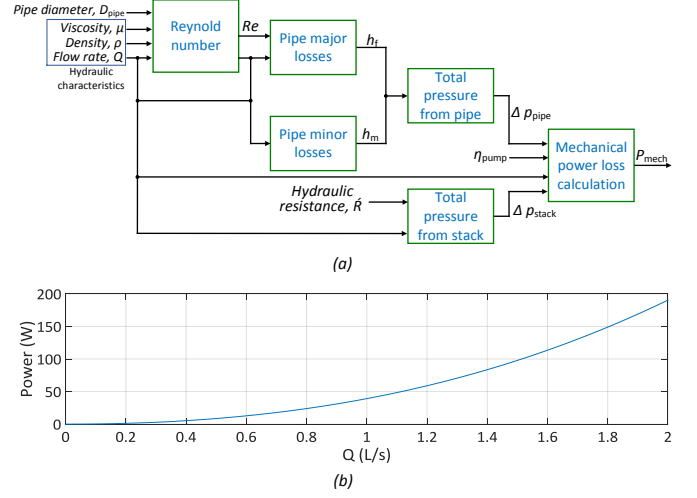


Fig. 6. (a) Mechanical losses block diagram [16] (b) Simulated pump power consumption with different electrolyte flow rates

the expense of higher pump power consumption, which can potentially compromise the overall VRB system efficiency. The ideal approach is to vary the electrolyte flow rate to track the optimal operating points. However, since the efficiency map was generated experimentally at a constant flow rate of 2 l/s [15], this fixed value (and consequent fixed pump loss) was adopted in the simulation setup at this stage.

IV. NAÏVE EMS

Our initial proposed control strategy for the HESS is a simple rule-based and filter-based approach shown in Fig. 7 and Fig. 8. The rule-based controller decides whether the VRB system should be used at all by evaluating the energy surplus/deficit within the overall off-grid system. From Fig. 6(b), the pump power consumption is about 190 W when the flow rate is fixed at 2 l/s. This means that the VRB system is not economical when used below this power level. For simplicity, the threshold value was set at a higher value of 500 W to prevent the VRB operating in a low efficiency region. If the VRB system is being used, the controller further ensures that the power flow does not exceed its maximum power capability. When the VRB system reaches this limit, the remaining power flow must be met by the LIB. In this study, the upper threshold value was set at 2 kW to give a buffer for the VRB system, which has a fast response, to absorb any additional power fluctuations from the PV generation or load demand thus minimising throughput of the LIB battery. This was achieved by a filter-based method which diverts the high frequency components of the power demand to the VRB and low frequency variations to the LIB, as shown in Fig. 8.

The system shown in Fig. 2 was simulated in Matlab/Simulink and the results are given in Fig. 9. The first plot shows the power generation from the PV system (rated at 5 kW peak). Variations in solar irradiation were emulated and the proposed controller was verified in diverting the high frequency fluctuations to the VRB system when it was in operation. At the start of the simulation, PV generation increased

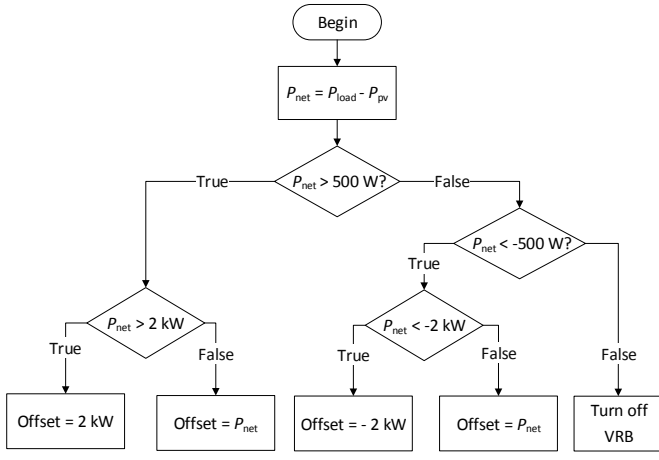


Fig. 7. Flowchart of the rule-based control

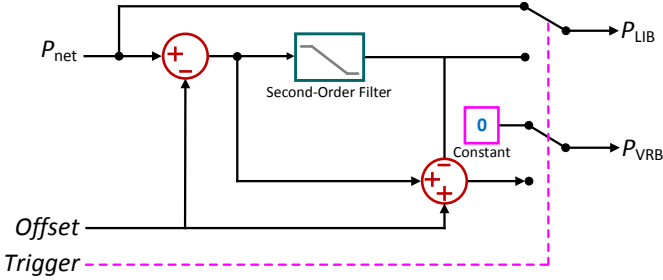


Fig. 8. Filter-based control

linearly while loads were switched-off. At approximately 20 s, the VRB system reached its charging power limit of 2 kW. It was maintained at this level with perturbations being observed when the load was turned-on at 60 s. The LIB absorbed the additional power generated from the PV system. However, the filter has a slow transient response as seen in these results. At 80 s, the load demand closely matches the PV generation. As expected, the VRB does not operate at this point, and the LIB supports the system instead. As the load further increases, the VRB system is first used as it has a higher durability. Nonetheless, the LIB is then required to meet the high power demand when the PV generation decreases significantly.

V. OPTIMAL EMS

As mentioned in the introduction, the proposed HESS leads to a multi-objective problem: minimising losses in the VRB and LIB, L_{VRB} and L_{LIB} , versus minimising li-ion battery degradation, D_{LIB} , forming the cost function given in equation (9) below. The power demands of the load, $Q_{load}(t)$, and the PV production, $Q_{pv}(t)$, have to be met using the VRB, $Q_{VRB}(t)$, and the LIB, $Q_{LIB}(t)$, (10). The losses in the VRB (11) are the sum of stack losses, assumed to be proportional to the absolute value of the VRB power at time t , $|Q_{VRB}(t)|$, with a constant efficiency, η_{VRB} , and the pumping losses, Q_{pump} , which are multiplied with a binary variable, $O(t)$, indicating whether the VRB is on at time t (12). The losses of the LIB are proportional to the absolute value of the LIB power at time t , $|Q_{LIB}(t)|$, again with a constant efficiency, η_{LIB}

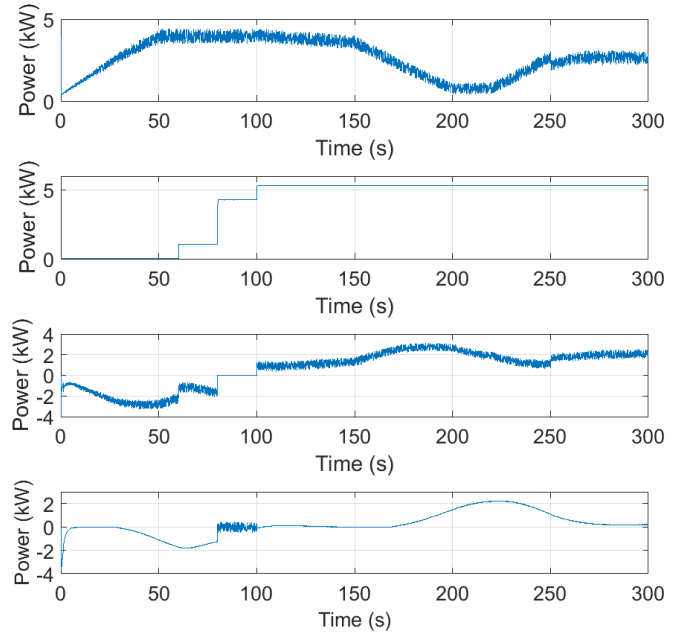


Fig. 9. Power flow simulation results, top to bottom: (a) PV generation, (b) load demand, (c) VRB power flow, (d) LIB power flow

(13). The degradation of the LIB is assumed to be proportional to the total energy throughput of the LIB (14). Both batteries are represented as simple energy ‘buckets’, where the state of charge (really, state of energy, but for simplicity we will call this state of charge) is the time integral of the power to or from the battery up to time t (15). At all times, the batteries’ SOC are constrained according to equation (16). Three control scenarios are considered here: only minimising losses ($\alpha = 1$), only minimising degradation ($\alpha = 0$) and a middle case where both losses and degradation are considered ($\alpha = 0.5$). To avoid frequent on/off switching, the VRB was required to have been on for at least 15 consecutive minutes before it could turn off again (17-18), where $S(t)$ is a binary variable indicating if the VRB switches on and hence has to remain on for the next 15 minutes. The full set of equations relating to this optimisation problem is as follows:

$$\min(\alpha(L_{VRB} + L_{LIB}) + (1 - \alpha) * D_{LIB}) \quad (9)$$

$$Q_{VRB}(t) + Q_{LIB}(t) = Q_{pv}(t) + Q_{load}(t) \quad (10)$$

$$L_{VRB} = \sum_t ((1 - \eta_{VRB}) |Q_{VRB}(t)| dt + Q_{pump} O(t) dt) \quad (11)$$

$$-Q_{VRB}^{max} O(t) \leq Q_{VRB}(t) \leq Q_{VRB}^{max} O(t) \quad (12)$$

$$L_{LIB} = \sum_t ((1 - \eta_{LIB}) |Q_{LIB}(t)| dt) \quad (13)$$

$$D_{LIB} = c * \sum_t (|Q_{LIB}(t)| dt) \quad (14)$$

$$SOC_i(t) = SOC_{ini} + \int_{z=0}^t Q_i(z) dz \quad (15)$$

$$10\% \leq SOC_i(t) \leq 90\% \quad (16)$$

$$O(t) \leq \sum_{z=t-14}^t S(z) \quad (17)$$

$$15S(t) \leq \sum_{z=t}^{t+14} O(z) \quad (18)$$

This is a mixed-integer linear problem, where the integers are the binary variables indicating whether the VRB is on or not. For one set of weights, it can be solved using standard solvers such as CBC or GLPK.

VI. SIMULATION RESULTS AND DISCUSSION

This section aims to compare the naïve vs. optimal EMS approaches of the HESS. The former adopted a rule-based approach ('base case') whilst three cases (only considering degradation, consider both degradation and losses, and only considering losses) were formulated using the latter. The simulation methodology was described in Section II. Fig. 10 shows the power flow within the system (naïve approach) occurred throughout the day. From Fig. 10a, it is noticed that the solar irradiance (and hence the PV power generation) was highly fluctuating, which may be associated with fast moving clouds [8]. In the meanwhile, the load demand which was synthesised for three dwellings exhibits high electricity usage during the midday and evening [9]. Between 12 am and about 6am, the load demand was solely met by the LIB when the magnitude was less than 500 W. At about 7 am, the PV panels started to generate electricity and the load demand increased to slightly more than 3 kW. Since the net power between the load and generation during that hour is more than 2 kW, the VRB system (Fig. 10b) tried to maintain its power at that level (from the defined rule) whilst the LIB (Fig. 10c) supplied remaining power requirement. It is also noticed that most of the PV fluctuations was absorbed by the VRB system.

In many instances between 10 am and 3 pm, the HESS was in charging mode due to the PV generation. However, it is noticed that the VRB charging power frequently exceeded the pre-defined maximum power set-point of 2 kW. To further illustrate this, Fig. 10(d) shows a zoomed in section of operation in the middle of the day. In general, the rate of change of the VRB power (in blue) is similar to the PV generation (in orange) whereas the LIB charging power (in green) is smoother due to the filter. However, four noticeable VRB power peaks (more than 4 kW) are observed in this short period, especially when there were sudden increases of PV generation (from about 2 kW to 5 kW). These scenarios are associated with the low-pass filter's phase delay effect which

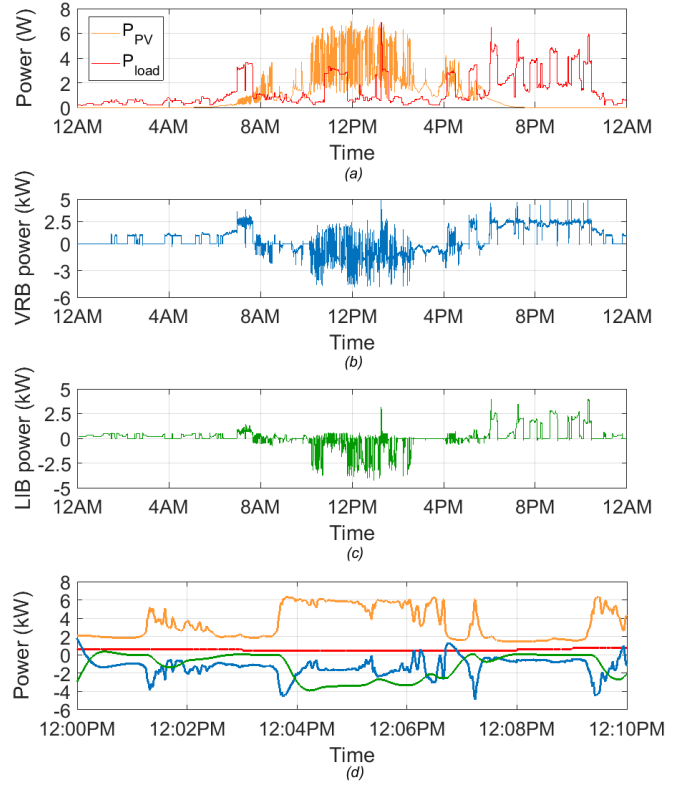


Fig. 10. Simulation results of naïve approach over 24 hours: (a) PV generation and load demand, (b) VRB power flow, (c) LIB power flow, (d) Ten minutes zoomed-in power flows

diverted the low frequency variations to the LIB. Because at all times the power balance within the off-grid system has to be fulfilled, whilst there are no other backup sources, the VRB system was required to meet the power requirement as the rate of change of the LIB power was lower. To overcome this issue, the bandwidth of the filter may be increased to allow LIB to react quicker but this also means that it would be susceptible to more power fluctuations. This can be regarded as a trade-off and more advanced filter design is required to mitigate this problem, or an increase in dc link capacitance. Nevertheless, the 10-minutes averaged power of the VRB system is -1.81 kW, which is still within the specified average power (Table I). Similar explanations can be applied to the VRB discharging power spikes observed in the evening, which were mainly due to the load switching.

In contrast, simulations of the optimal control results of the HESS for the three considered scenarios are shown in Fig. 11, Fig. 12 and Fig. 13 respectively. The simulation results from both the high fidelity and low fidelity models are plotted for comparison purposes. Greater discrepancies lie within the VRB power flows compared to the LIB. This may be attributed to the lower sampling rate of the optimisation model, as well as the assumptions made in the model, i.e. using constant VRB efficiency and treating the batteries as linear systems. Nevertheless, the HESS in the Simulink operated stably based on the optimised power set-points. As expected, when the objective function was to minimise degradation, the VRB was

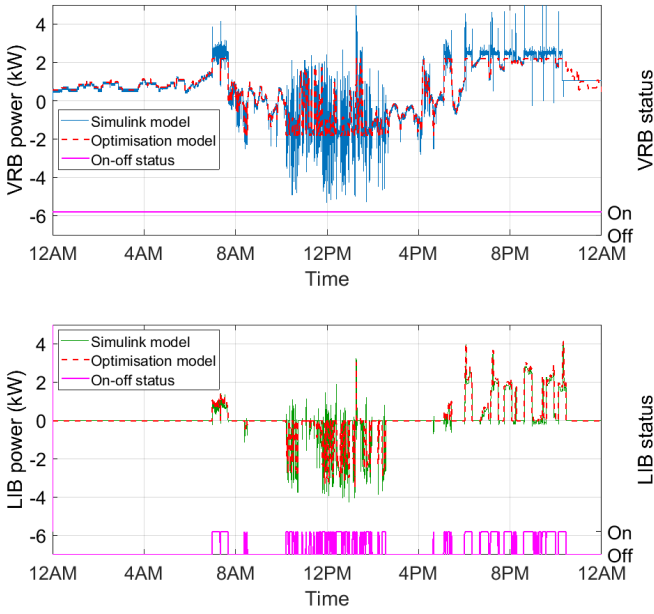


Fig. 11. Optimal (a) VRB power flow, (b) LIB power flow by minimising only degradation

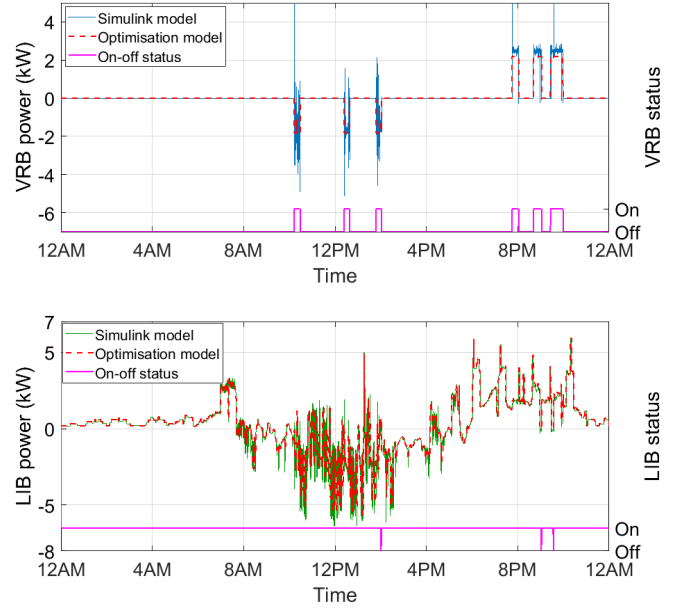


Fig. 13. Optimal (a) VRB power flow, (b) LIB power flow operations by minimising only power losses

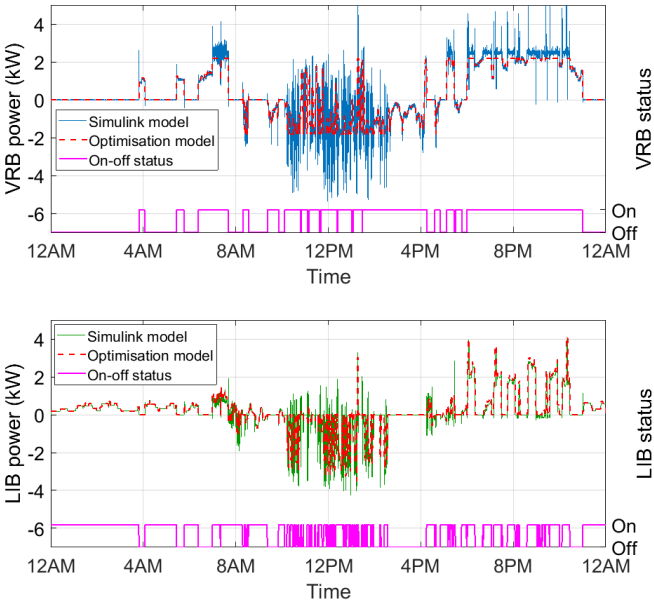


Fig. 12. Optimal (a) VRB power flow, (b) LIB power flow by minimising both degradation and power losses

used almost exclusively, and the LIB supported the power deficit. The opposite situation occurred when the objective was to minimise power losses. When both degradation and power losses are considered, decisions are made based on the levelised costs associated with degradation and power losses (represented with different weighting factors, α). The results in Fig. 12 are generated based on α equals to 0.5 (both are equally priced).

The batteries SOC profiles for all four cases are shown in Fig. 14. Note that when minimising degradation was the main objective, the VRB was fully discharged despite the SOC

constraints being considered in the optimisation model. This can be attributed to the discrepancies between the optimisation and Simulink models which further highlight the importance of using the latter to verify the former. In reality, this problem may be avoided if more stringent SOC limits are used or by increasing the battery capacity. By simply comparing the SOC profiles and their corresponding depth of discharge, the batteries energy throughput can be also reflected. In the case of minimising degradation, the LIB was cycled less. When power losses was not the only consideration ($\alpha = 0.5$), partial charge-discharge cycles during the day (between 10 am to 3pm) was minimal which further demonstrates the advantage of hybridisation. The cumulative loss plots for both batteries are shown in Fig. 15. It is interesting to note that the optimal approach ($\alpha = 0.5$) marginally outperformed the naïve approach but they are, perhaps by coincidence, remarkably similar. In practice, one may choose to use the latter if accurate forecasts of renewables and load demands are not available.

VII. CONCLUSION

This paper explores through simulations the application of a hybrid VRB-LIB ESS for an off-grid renewable power system. The objective was to demonstrate the efficacy of two different control strategies for this system: first, a simple rule-based and filter-based control strategy, and second, a more complex optimisation based strategy, each with the aim to trade-off between the advantages and disadvantages of the two energy storage devices. The VRB is known to have non-negligible parasitic losses, which mean that operation at low power levels is inefficient, but it has an extremely long life and a fast response rate. On the contrary, the LIB is generally an efficient device but lifetime is smaller than the VRB, and rapid fluctuations may be detrimental. We showed that the

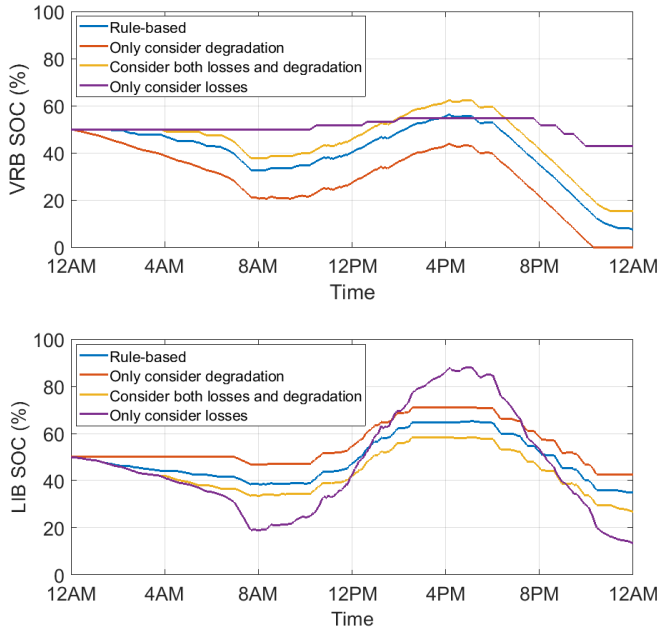


Fig. 14. SOC comparison of the naïve and optimal EMS approaches

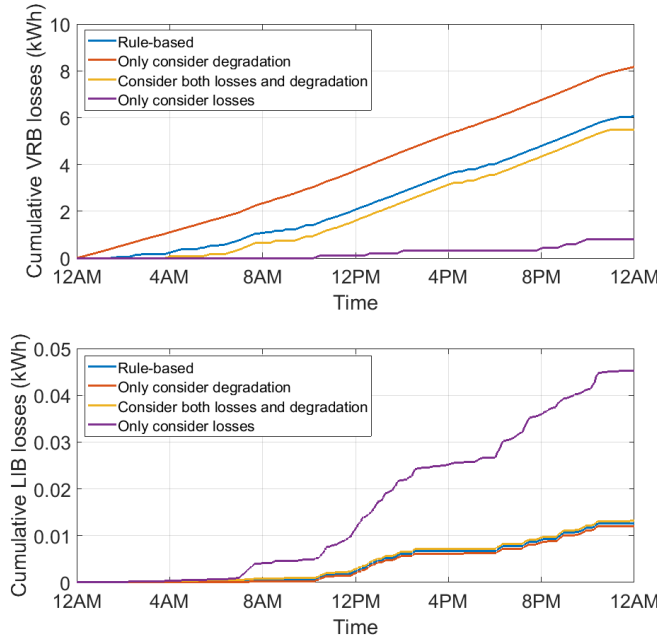


Fig. 15. Cumulative energy losses comparison of the naïve and optimal EMS approaches

simple control approach works reasonably well, but due to the transient response of the filter used to divert higher frequency power fluctuations to the VRB, there can be unintended large and unrealistic power peaks on the system. The optimisation based approach included a factor, α , allowing the user to set as a priority either efficiency (which favours using the LIB) or minimising degradation (which favours VRB operation), or some mixture of the two. In terms of overall power losses over a 24 hour high fidelity simulation, the simple ruled based method performed similarly to an optimal strategy that tried to

equally weight efficiency and degradation. Future work might consider more realistic models of LIB degradation, and verification of the various control strategies against experimental results.

ACKNOWLEDGEMENT

This work was supported by the Korea Institute of Energy Technology Evaluation and Planning (KETEP) and the Ministry of Trade, Industry and Energy (MOTIE) of the Republic of Korea (No. 20148510011150). Jorn Reniers is supported by VITO and EnergyVille.

REFERENCES

- [1] M. Ismail, M. Moghavvemi, and T. Mahlia, "Techno-economic analysis of an optimized photovoltaic and diesel generator hybrid power system for remote houses in a tropical climate," *Energy Conversion and Management*, vol. 69, pp. 163–173, 2013.
- [2] Y. Kim, J. Koh, Q. Xie, Y. Wang, N. Chang, and M. Pedram, "A scalable and flexible hybrid energy storage system design and implementation," *Journal of Power Sources*, vol. 255, pp. 410–422, 2014.
- [3] H. Zhou, T. Bhattacharya, D. Tran, T. S. T. Siew, and A. M. Khambadkone, "Composite Energy Storage System Involving Battery and Ultracapacitor With Dynamic Energy Management in Microgrid Applications," *IEEE Transactions on Power Electronics*, vol. 26, no. 3, pp. 923–930, mar 2011.
- [4] A. M. Gee, F. V. P. Robinson, and R. W. Dunn, "Analysis of Battery Lifetime Extension in a Small-Scale Wind-Energy System Using Supercapacitors," *IEEE Transactions on Energy Conversion*, vol. 28, no. 1, pp. 24–33, 2013.
- [5] C. Doetsch and J. Burfeind, "Chapter 12 Vanadium Redox Flow Batteries," in *Storing Energy*, 2016, pp. 227–246.
- [6] P. Kurzweil, "Chapter 16 Lithium Battery Energy Storage: State of the Art Including LithiumAir and LithiumSulfur Systems," in *Electrochemical Energy Storage for Renewable Sources and Grid Balancing*, 2015, pp. 269–307.
- [7] M. Skyllas-Kazacos, M. H. Chakrabarti, S. A. Hajimolana, F. S. Mjalli, and M. Saleem, "Progress in Flow Battery Research and Development," *Journal of The Electrochemical Society*, vol. 158, no. 8, pp. R55–R79, 2011.
- [8] "High-Resolution Solar Radiation Datasets." [Online]. Available: <http://www.nrcan.gc.ca/energy/renewable-electricity/solar-photovoltaic/18409>
- [9] E. McKenna and M. Thomson, "High-resolution stochastic integrated thermalelectrical domestic demand model," *Applied Energy*, vol. 165, pp. 445–461, 2016.
- [10] I. Richardson, M. Thomson, D. Infield, and C. Clifford, "Domestic electricity use: A high-resolution energy demand model," *Energy and Buildings*, vol. 42, no. 10, pp. 1878–1887, 2010.
- [11] L. K. Gan, J. K. Shek, and M. A. Mueller, "Modelling and experimentation of grid-forming inverters for standalone hybrid wind-battery systems," in *International Conference on Renewable Energy Research and Applications (ICRERA)*, 2015, pp. 449–454.
- [12] L. J. Ontiveros and P. E. Mercado, "Modeling of a Vanadium Redox Flow Battery for power system dynamic studies," *International Journal of Hydrogen Energy*, vol. 39, no. 16, pp. 8720–8727, 2014.
- [13] J. Lopes, C. Moreira, and A. Madureira, "Defining Control Strategies for MicroGrids Islanded Operation," *IEEE Transactions on Power Systems*, vol. 21, no. 2, pp. 916–924, 2006.
- [14] E. Koutroulis, K. Kalaitzakis, and N. Voulgaris, "Development of a microcontroller-based, photovoltaic maximum power point tracking control system," *IEEE Transactions on Power Electronics*, vol. 16, no. 1, pp. 46–54, 2001.
- [15] M. Skyllas-Kazacos and C. Menictas, "The vanadium redox battery for emergency back-up applications," in *Proceedings of Power and Energy Systems in Converging Markets*, 1997, pp. 463–471.
- [16] C. Blanc, "Modeling of a vanadium redox flow battery electricity storage system," Ph.D. dissertation, École polytechnique fédérale de Lausanne (EPFL), 2009.
- [17] Y. Zhang, J. Zhao, P. Wang, M. Skyllas-Kazacos, B. Xiong, and R. Badrinarayanan, "A comprehensive equivalent circuit model of all-vanadium redox flow battery for power system analysis," *Journal of Power Sources*, vol. 290, pp. 14–24, 2015.